

**Correction to: Determination of transfer stress from ruptured pre-load galvanised tendons in tanks and bund walls**

O'FLAHERTY, Fin <<http://orcid.org/0000-0003-3121-0492>>, LAMBERT, Paul, MANGAT, Pal <<http://orcid.org/0000-0003-1736-8891>> and STARINIERI, Vincenzo <<http://orcid.org/0000-0002-7556-0702>>

Available from Sheffield Hallam University Research Archive (SHURA) at:

<http://shura.shu.ac.uk/24105/>

---

This document is the author deposited version. You are advised to consult the publisher's version if you wish to cite from it.

**Published version**

O'FLAHERTY, Fin, LAMBERT, Paul, MANGAT, Pal and STARINIERI, Vincenzo (2019). Correction to: Determination of transfer stress from ruptured pre-load galvanised tendons in tanks and bund walls. *Materials and Structures*, 52 (1).

---

**Copyright and re-use policy**

See <http://shura.shu.ac.uk/information.html>

# Determination of transfer stress from ruptured pre-load galvanised tendons in tanks and bund walls

Fin O'Flaherty  · Paul Lambert  · Pal Mangat  · Vincenzo Starinieri 

Received: 12 July 2017 / Accepted: 19 September 2017 / Published online: 5 October 2017  
© RILEM 2017

**Abstract** Circular concrete tanks and containment bunds constructed by the pre-load method involves pre-stressing the concrete by repeatedly wrapping layers of highly tensioned tendons. Each layer is covered with gunite. Corrosion may lead to rupture and an explosive type failure is avoided if the gunite is able to absorb the transfer stress. Zinc galvanizing is used to increase the tendons resistance to corrosion but its smoothness can influence bond characteristics, as can corrosion if extensive. This paper investigates the pre-stress transfer of ruptured pre-load tendons in gunite, both in the uncorroded and corroded state. Laboratory testing was conducted where tendons were pre-loaded in custom-built stressing moulds (to 1000 MPa) and simulated gunite applied. Different degrees of accelerated corrosion were applied to the tendons (0–10%). The bond stress at transfer was determined by measuring the contraction of the tendon during release of the pre-stress (replicating a broken tendon). The results show that a low bond stress was found either as a result of the smooth zinc coating (uncorroded tendons) or due to higher levels of corrosion. These results were compared to design equations from Eurocode 2 and recommendations are

made for reducing the bond coefficient  $\eta_{p1}$ , the coefficient that takes into account the type of tendon and the bond situation. Analysis is subsequently conducted to determine the transfer stress in the gunite by modelling single and double tendon ruptures and establishing the magnitude of compressive stress which, if excessive, may lead to an explosive type failure of the gunite.

**Keywords** Corrosion · Pre-load tendons · Rupture · Bond · Galvanized steel · Gunite cover · Explosive failure

## List of symbols

$A_t$	Cross-sectional area of the tendon
$A_{\text{eclipse}}$	Area of eclipsed zone of influence from pre-stress transfer from two adjacent ruptured tendons
$A_{g(\text{eclipse})}$	Net area of gunite in the eclipsed zone from pre-stress transfer from two adjacent ruptured tendons
$A_{g(\text{equiv})}$	Equivalent area of gunite calculated from the modular ratio between the tendon and gunite
$A_{\text{ring}}$	Area of the zone of influence minus the area of the ruptured tendon
$A_{\text{zone}}$	Area of the zone around a tendon influenced by a transfer of pre-stress due to rupture
$a$	Surface area of steel

F. O'Flaherty (✉) · P. Lambert · P. Mangat · V. Starinieri  
Centre for Infrastructure Management, Materials and Engineering Research Institute, Sheffield Hallam University, Howard Street, Sheffield S1 1WB, UK  
e-mail: f.j.oflaherty@shu.ac.uk

$\alpha_{ct}$	Coefficient accounting for long term effects on tensile strength of concrete/gunite	$n$	Number of effective tendons in zone of influence in addition to the ruptured tendon
$\alpha_1$	Coefficient for sudden release of pre-stress	$\sigma_{bpt}$	Pre-stress transfer
$\alpha_2$	Coefficient for tendons with circular cross section	$\sigma_{pm0}$	Tendon stress just after release
$\gamma_c$	Partial safety factor for concrete/gunite	$M$	Percentage of material mass loss due to corrosion
$C_t$	Gunite cover to the ruptured tendon	$R$	Material loss per year due to corrosion
$\Delta_{bpt}$	Contraction of pre-stressed tendon after release	$r$	Radius of bund wall or tank
$E_g$	Modulus of elasticity of gunite	$T$	Time in years
$E_t$	Modulus of elasticity of tendon	$\emptyset_t$	Nominal diameter of tendon
$F_g$	Force transferred to the gunite after tendon rupture	$\emptyset_{t(corr)}$	Reduced diameter of the corroded tendon
$F_t$	Pre-stressing force in the tendon	$\emptyset_{t(red)}$	Reduction in tendon diameter due to corrosion
$F_{fr}$	Loss of prestressing force due to friction	$\emptyset_z$	Diameter of zone of influence after tendon rupture
$F_{net}$	Net force in the tendon after frictional losses		
$f_{bpt}$	Bond stress between tendon and gunite		
$f_{ctd}(t)$	Design tensile value of strength of concrete/gunite at time of pre-stress release		
$f_{ctm}(t)$	Tensile strength of concrete/gunite at time $t$		
$f_{cu}$	Compressive strength of concrete/gunite		
$f_g$	Stress in the gunite after pre-stress transfer from ruptured tendon		
$f_g(eclipse)$	Additional pre-stress transfer to the eclipsed zone of influence in the gunite due to rupture of an adjacent (second) tendon		
$f_t$	Stress in the ruptured tendon beyond the transmission length		
$f_{t(uts)}$	Ultimate tensile strength of a tendon		
$\eta_{p1}$	Coefficient accounting for the type of tendon and the bond situation at release		
$\eta_1$	Coefficient for bond conditions at release		
$\theta$	Subtended angle from the centre of the bund to the extremities of the transmission length		
$I$	Corrosion current		
$i$	Corrosion current density		
$L$	Length of steel		
$l_{pt}$	Transmission length at pre-stress transfer		
$m$	Modular ratio between tendon and gunite		
$\mu$	Coefficient of friction between steel and gunite		

## 1 Introduction

Pre-stressed concrete storage tanks and bund walls, sometimes referred to as preload or wire wound concrete tanks and bunds, were a common structure from the 1950s to 1970s, with the last being built in the UK in 1981 for providing water storage tanks and secondary confinement around liquid storage tanks in the event of spillage. It was a patented system [1] for banding tanks more efficiently and with less expenditure of time, labour and materials. The method uses a tendon carrying-and-placing vehicle supported for movement around and adjacent to the outer face of the tank to be banded. One end of the tendon is anchored at a starting point and the tendons are circumferentially wrapped around the concrete structure in layers. Applied in a helical process, the pre-stressing tendon is most commonly wrapped in a recess to form bands, with each layer receiving a coating of spray applied gunite. By covering each wire, the aim is to provide a durable and fully bonded pre-stressing system. Circumferential pre-stressing maintains the concrete in a state of compression so tensile cracks are eliminated. The tank or bund wall is wrapped to an initial maximum compressive stress of about 55%  $f_{cu}$  and a final design compressive stress of about 45%  $f_{cu}$  is achieved after pre-stressing losses.

The actual stress in the wire is accurately measured during winding to ensure that the applied pre-stressing

force is in accordance with the design. The layers continually build up until the final gunite covering is floated to provide a flush surface and an aesthetically pleasing appearance. The tendons can be coated with zinc galvanizing, as was commonly the case in the United Kingdom, but corrosion has become an issue in some structures meaning the strength of the tendon and bond strength can be severely compromised. Pre-load tendons can be stressed up to 60% of their ultimate tensile strength, and because their diameter is nominally only about 5 mm, a loss in cross-sectional area due to corrosion can increase the stress level considerably. A reduction in cross-sectional area of a wire can exceed 30% after only 20 years of corrosion propagation even at low corrosion rates [2]. In addition, the anodic dissolution of tendons accelerates with the increasing tensile stress [3].

Coatings such as hot-dip galvanizing are used to improve corrosion resistance and is recognized as an effective protection measure for pre-stressing steels [4] with many publications on its performance [5–8]. Of the several corrosion protection systems that are available [9], zinc and zinc-based (e.g. zinc-aluminium) coating systems are the most common [4, 10]. However, zinc and aluminium are sensitive to the high alkaline environment of wet cement mortar or concrete [11]. As a consequence of zinc corrosion, hydrogen may develop and hydrogen-induced failures of pre-stressing steel may occur [4]. However, there is evidence to the contrary where a 40 year old bridge showed deterioration mainly due to insufficient concrete cover to the tendons instead of stress corrosion or hydrogen embrittlement [12]. Despite the attention being given to corrosion and hydrogen generation which may lead to failure of the tendon, the interaction between a ruptured tendon and surrounding gunite has not been fully established and its significance is discussed in the following section.

## 2 Research significance

The boom in the construction of pre-load tanks and bund wall containment structures from the 1950s onwards means that these structures are now at an age where deterioration due to corrosion of the pre-stressing steel is a distinct possibility (further information on typical repair techniques is available [13]). Since the purpose of the wrap-around band is to

provide circumferential pre-stress to keep the bund wall in compression to about 45%  $f_{cu}$ , it is unlikely that the localised rupture of one or two tendons will have an appreciable effect on the strength as long as the tendon can transfer full pre-stress (beyond the transmission length) to the gunite via bond around the circumference of the tank or bund wall. What is of significance is the potential for a localised explosive type failure when the tendon ruptures and there is insufficient area of gunite to absorb the energy. This has health and safety implications for operatives working near the bund wall as the explosive failure is normally sudden and without warning. The analysis provided in this paper will enable the inspection engineer to assess the likelihood of an explosive type failure by gathering design, construction and in-service information such as cover to gunite, magnitude of pre-load, diameter and type of tendon and likely areas of corrosion and using these to estimate the transfer stress to the gunite at rupture of one or more tendons.

The analysis, where required, is related to design equations from Eurocode 2 [EC2, 14] e.g. determination of bond stress and transmission length at pre-stress transfer (rupture of the tendon). However, EC2 accommodates two types of pre-stressing steel, indented wire and three & seven wire strands. Tanks and bund walls constructed in the 1950s–1970s used galvanised, 5 mm (or imperial equivalent) high strength tendons hence information on the bond between smooth, galvanised tendons, both with and without corrosion, was required before the recommendations in EC2 could be utilised. A series of laboratory bond tests were conducted and these are outlined in the next section.

## 3 Materials and methods

### 3.1 Preparation of moulds and test specimens

A number of timber moulds/pre-stressing beds (Fig. 1) were designed and developed to (1) pre-load the tendon; (2) provide formwork for the 100 mm × 100 mm mortar formulated to represent gunite in composition and strength (hereafter referred to as gunite) and (3) enable the magnitude of pre-stress transfer to the gunite to be determined at rupture. The

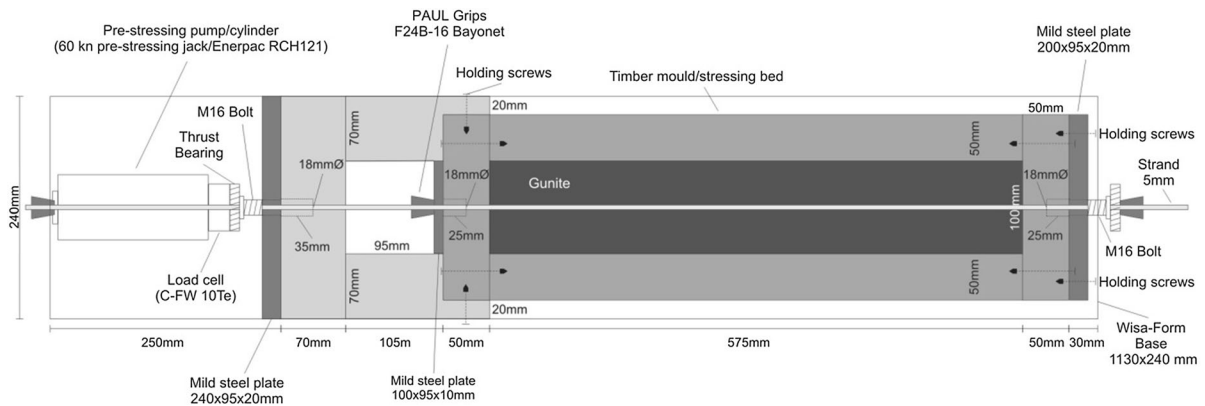


**Fig. 1** Timber mould and stressing bed

main components of the test system are given in Fig. 1.

The internal length of the timber mould was 575 mm (Fig. 1), based on a transmission length of at least 100 diameters, albeit it for indented wires in EC2 [15] (tendon diameter in this study was nominally 5.4 mm as it was not possible to source 5 mm galvanised tendons as was typically used in the original construction). Twelve moulds were manufactured and used three times for casting batches labelled A, B and C. The removable loading apparatus was attached in turn to each mould to apply a pre-determined load to the tendon via the hollow cylinder.

Wedges were used at both ends to maintain the pre-load in the tendon. Pre-loading of the tendon was conducted at least one day before casting to allow relaxation to occur before the gunite was applied. Some slippage occurred during release of the loading system so some variation in pre-load was to be expected (the actual pre-stress transfer was determined by measuring the ‘shrink-length’ upon release of load as described in Sect. 3.5). The cast specimens were stored under polyethylene sheeting in the laboratory. Four specimens per batch were used as control specimens (0% corrosion), the remaining eight were exposed to various degrees of tendon corrosion (up to 10% mass loss).

### 3.2 Details of tendons and gunite composition

The galvanized tendons selected for testing had a diameter of 5.4 mm with a  $\sim 30 \mu\text{m}$  galvanizing layer of zinc. Before casting, all tendons were weighed to confirm metal loss due to corrosion at the end of testing.

A sand/cement mortar of ratio 5:1 was used to represent the gunite based on the compositional analysis of samples taken from existing pre-load structures ( $f_{cu} \sim 35 \text{ MPa}$ ). Ordinary Portland cement (OPC), supplied by Castle Cement Ltd, Lincolnshire, UK was used in the gunite. The cement content was  $340 \text{ kg/m}^3$  (w/c ratio  $\sim 0.2$ ). Fine aggregate was medium grade sand according to BS EN 12620:2013 [16]. No other admixtures were used. Compaction was carried out with a 25 mm square tamping bar as the dry sprayed application method was considered impractical with small moulds in a laboratory environment. Special attention was given to achieving full compaction around the tendon, especially the area behind it.

### 3.3 Accelerated corrosion of tendons

Following a 2 weeks curing period of the gunite, the tendon in each specimen was subjected to general corrosion by applying an anodic impressed current provided by a DC power supply. Different percentages of corrosion were selected following trials from 0 (control) to 10%. Applying a unit degree of corrosion ( $M = 1\%$ ), the following equations were used to determine the time taken to achieve 1% corrosion:

$$\begin{aligned} \frac{2RT}{\phi_t} &= \frac{M}{100} \rightarrow R = \frac{M\phi_t}{2(100)T} = \frac{M\phi_t}{200T} = 1165i \rightarrow T \\ &= \frac{M\phi_t}{200(1165i)}. \end{aligned} \quad (1)$$

A current density,  $i$ , of  $0.5 \text{ mA/cm}^2$  was used to simulate general corrosion. This current density was

previously adopted in earlier experiments and was found to provide an appropriate level of corrosion within a reasonable timescale [17]. Inserting  $i = 0.5 \text{ mA/cm}^2$ ,  $\phi_t = 0.54 \text{ cm}$  and  $M = 1\%$  into Eq. 1 gives:

$$\frac{(1)(0.54)}{(200)(0.5825)} = 0.00463 \text{ years} = 1.692 \text{ days} \\ = 40.6 \text{ h/1\% corrosion.} \quad (2)$$

The length of tendon surrounded by gunite is 57.5 cm (Fig. 1). The total surface area,  $a$ , of the tendon is:

$$a = \pi \phi_t L = 31.05\pi \text{ cm}^2 \quad (3)$$

Therefore, the current required for 1% degree of corrosion is obtained from:

$$I = ia = (0.5)(31.05\pi) = 48.8 \text{ mA per specimen.} \quad (4)$$

Eight specimens were laid side-by-side in the laboratory for accelerated corrosion (Fig. 2) and current applied in parallel via a power supply. The polarity of the current was such that the tendon served as the anode and strips of mixed-metal oxide (titanium) placed on top of the specimens and weighed down to ensure full contact with the gunite



**Fig. 2** Accelerated corrosion of tendons via power supply (top left)

served as the cathode. The specimens were covered with a green landscaping fabric which was continuously moistened to maintain an electrolytic connection. For each batch of eight specimens, the applied current was fixed ( $48.8 \text{ mA} \times 8$ , Eq. 4) and corrosion period was adjusted (Eq. 2) to give the required target degree of corrosion (e.g. 121.8 h for 3%, 243.6 h for 6%).

In some cases, a longitudinal crack appeared along the top of the specimen for higher corrosion cases. When this was noticed, the corrosion current was switched off and the degree of corrosion was taken as the loss in cross sectional area to that point of the test (verified by reweighing after bond testing as described in Sect. 3.5).

### 3.4 Test schedule

The main variables which are considered to influence bond strength are the degree of corrosion in the tendons and their levels of pre-stress. The target level of pre-load (pre-stress) varied between 200 and 1000 MPa, the range easily covering typical prestresses as encountered in real structures (lower prestresses were investigated for comparative purposes). The target degree of corrosion ranged between 0% (control) to 10%. Thirty-six specimens were cast in three batches labelled A1–A12, B1–B12 and C1–C12.

### 3.5 Pre-stress transfer

The mould and stressing bed shown in Fig. 1 was used to determine the transfer of pre-stress to the gunite. The mould was securely fastened to the bed of a test frame and the pre-load was quickly released at one end by turning the mild steel bolt to relieve the stress in the tendon. The wedge was held with a vice-grip during stress release to prevent rotational bond failure of the tendon in the gunite. The contraction of the tendon was accurately measured via a linear variable displacement transducer (LVDT, accuracy calibrated using slip gauges) to give the ‘shrink-length’ upon release from which the transfer stress could be calculated.

Upon release of the pre-load, the tendons were removed from the gunite. The tendons were cleaned with 10% diammonium hydrogen citrate solution and reweighed to calculate the mass loss and determine the actual percentages of corrosion.



## 4 Laboratory results

### 4.1 Metallurgical testing

A visual representation of two different corrosion levels are given in Fig. 3. Referring to Fig. 3a, Sample A5 is considered as a Medium level of corrosion ( $\sim 3\%$ ) whereas Sample A11 in Fig. 3b represents a High level of corrosion ( $\sim 6\%$ ).

Both conditions represent the appearance of galvanized wires observed in pre-load structures. The Medium level of corrosion shows a significant proportion of white corrosion product from the galvanizing layer, with relatively little brown corrosion product from the underlying steel, Fig. 3a. At the Medium level, the loss of steel cross-section is minimal and the strength of the tendon relatively unaffected. The High level of corrosion represents the condition where corrosion of the steel substrate dominates, resulting in both higher volume corrosion products and reduction in the cross-section of the wire and is a precursor to the disruption of the gunite and possible failure of the wire, Fig. 3b.

### 4.2 Magnitude of pre-stress transfer

The results of the measured transfer of pre-stresses are given in Table 1. The specimen identification is given in Col. 1 and are listed in terms of increasing corrosion. Data from a total of 32 samples is given, four samples were excluded due to missing data. The

first twelve samples are control i.e. 0% corrosion from each of batches A, B and C, Col. 2. The samples are divided into three corrosion groups, namely 0, 0–5 and 5–10%, Col. 3. The measured contraction (or ‘shrink-length’,  $\Delta_{bpt}$ ) of the tendon upon transfer of pre-stress is given in Col. 4 from which the stress transfer ( $\sigma_{bpt}$ ) is calculated in Col. 5 [from  $\sigma_{bpt} = (E_t)(\Delta_{bpt}/L)$  where  $E_t$  is 289 kN/mm<sup>2</sup> (obtained from the supplier and verified in the laboratory) and L is the distance between anchorages, 735 mm].

The transfer of pre-stress ranged between 236 and 1140 MPa. This transferred pre-stress ( $\sigma_{bpt}$ ) may be assumed to be transferred to the gunite by a constant bond stress, the magnitude of which is shown in Col. 6 [ $f_{bpt} = (\sigma_{bpt})(A_t)/(\pi)(\phi_t)(L)$  where  $\phi_t$  is 5.4 mm and L is 575 mm]. For simplicity,  $\phi_t$  is taken as 5.4 mm for all calculations irrespective of the degree of corrosion.

The data presented in Cols. 2 and 6 in Table 1 is shown graphically in Fig. 4. The degree of corrosion is zero for the first twelve control samples but increases to a maximum of 10.49% for Sample A8. Referring to Table 1, the average bond stress at transfer for Groups 0 and 0–5% corrosion are quite similar, 1.91 and 1.88 N/mm<sup>2</sup> respectively, hence low levels of corrosion have not significantly influenced pre-stress transfer. However, this decreases to 1.50 N/mm<sup>2</sup> for corrosion Group 5–10% as the higher levels of corrosion has a greater influence on bond stress. For comparison, the design bond stress at transfer for a Grade 35 concrete and indented wire using the same parameters as used in the gunite example is also shown

**Fig. 3** **a** Medium corroded sample A5 ( $\sim 3\%$ ), **b** high corroded sample A11 ( $\sim 6\%$ )

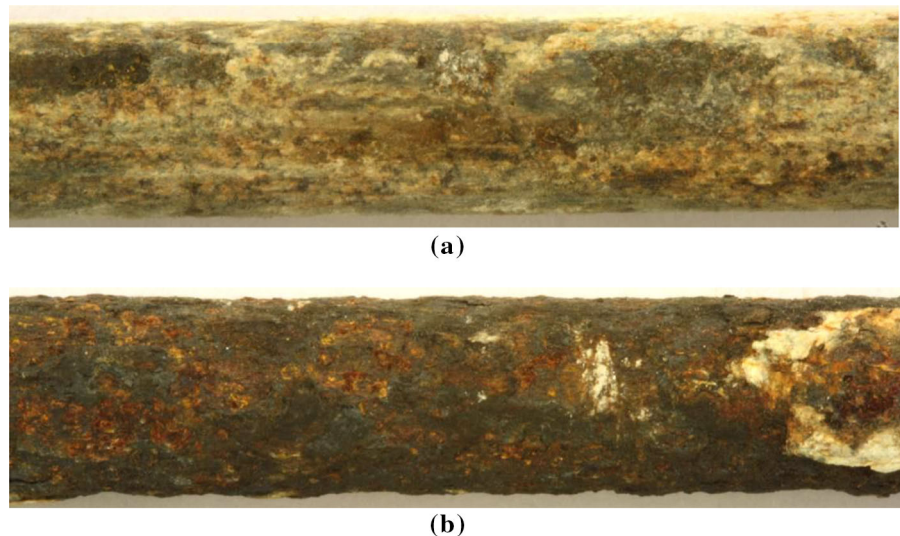


**Table 1** Bond strength of corroded tendons

1 ID	2 Actual corrosion (%)	3 Corrosion group (%)	4 Contraction upon pre-stress transfer, $\Delta_{bpt}$ (mm)	5 Calculated pre-stress transfer, $\sigma_{bpt}$ (MPa)	6 Calculated bond stress at transfer, $f_{bpt}$ (MPa)
A1	0.00	0	2.04	802	1.88
A2	0.00		1.73	680	1.60
A4	0.00		1.98	779	1.83
A6	0.00		2.46	967	2.27
B10	0.00		1.94	763	1.79
B11	0.00		1.70	668	1.57
B12	0.00		1.71	672	1.58
B9	0.00		1.72	676	1.59
C1	0.00		2.70	1062	2.49
C11	0.00		2.60	1022	2.40
C12	0.00		2.40	944	2.22
C2	0.00		1.90	747	1.75
Averages					1.91
A5	2.80	0–5	1.90	747	1.75
B8	3.82		1.02	401	0.94
B7	4.02		2.90	1140	2.68
C7	4.02		2.60	1022	2.40
B4	4.19		1.00	393	0.92
C6	4.28		2.60	1022	2.40
C5	4.29		2.20	865	2.03
C10	4.39		2.80	1101	2.58
A3	4.43		1.31	515	1.21
Averages					1.88
A10	5.10	5–10	1.75	688	1.62
C9	5.75		1.10	433	1.02
A9	5.84		0.60	236	0.55
C4	6.61		2.60	1022	2.40
C3	6.78		1.80	708	1.66
B6	7.72		2.09	822	1.93
B3	8.03		1.32	519	1.22
B2	8.59		2.15	845	1.98
A12	8.95		2.06	810	1.90
A7	9.41		1.10	433	1.02
A8	10.49		1.29	507	1.19
Averages					1.50

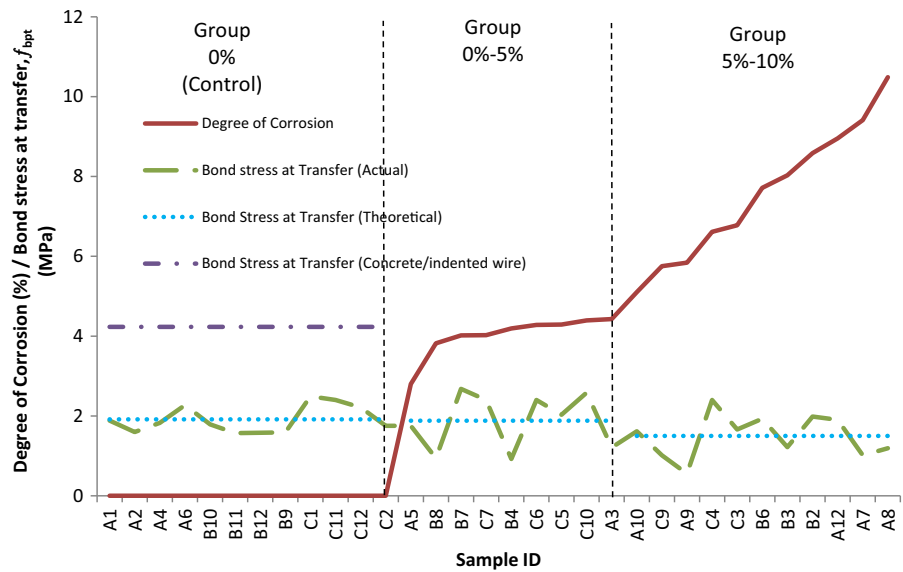
in Fig. 4 (0% corrosion,  $f_{bpt} = 4.23 \text{ N/mm}^2$ , also unfactored). This is significantly higher than the average bond stress for the pre-load tendon/gunite found in these tests ( $1.91 \text{ N/mm}^2$  at 0% corrosion,  $1.88 \text{ N/mm}^2$  at 0–5% corrosion and  $1.50 \text{ N/mm}^2$  at 5–10%).

## 5 Analysis of a ruptured pre-load tendon

When a tendon ruptures due to corrosion, an explosive type failure is avoided if the pre-stress transfer to the gunite, via bond, does not cause overstressing. Friction between the steel tendon and gunite/concrete, which is



**Fig. 4** Relationship between degree of corrosion and bond stress at transfer



considered a loss when designing conventional post-tensioned concrete, may reduce the magnitude of pre-load transfer into the gunite as a result of the tightly wound tendons (in the transmission length only). Consequently, the following sections will determine parameters for galvanised pre-load tendons that can be used to establish the impact of rupture of the pre-stressed tendons. Bond characteristics are given in Sect. 5.1. The frictional force between the tendon and gunite due to curvature will be determined in Sect. 5.2. The compressive stress in the gunite at pre-stress transfer from a single (Sect. 5.3) or double (Sect. 5.4) tendon rupture is determined which will establish if an explosive type failure of the gunite is possible. In Sects. 5.2–5.4, the analysis is clarified in the form of a worked example featuring as-designed and as-constructed parameters from an actual pre-load structure.

### 5.1 Transfer of pre-stress at rupture

The mechanism of pre-stress transfer in a ruptured wrap-around tendon can be compared to transfer in conventional pre-stressed concrete, the only difference being that the pre-stress release in conventional manufacture is carefully planned and managed whereas in pre-load tendons, it occurs without warning. Therefore, the design recommendations as given in EC 2 [14] are used as a basis for analysis. This part of the Eurocode clearly relates to pre-stressed concrete

structures but the equations will be applied here to accommodate transfer of pre-stress to gunite instead of concrete. According to EC 2 [14], Section 8.10.2.2 (1), the pre-stress at release of tendons may be assumed to be transferred to the concrete by a constant bond stress,  $f_{bpt}$ , given as:

$$f_{bpt} = (\eta_{p1})(\eta_1)(f_{ctd}(t)) \quad (5)$$

where  $\eta_{p1}$  is a coefficient that takes into account the type of tendon and the bond situation at release (2.7 for indented wires or 3.2 for three and seven wire strands, a value for plain, galvanised tendons is not given),  $\eta_1 = 1.0$  for good bond conditions or 0.7 otherwise, unless a higher value can be justified with regard to special circumstances in execution.

$f_{ctd}(t)$  is the design tensile value of strength at time of release:

$$f_{ctd}(t) = \frac{(\alpha_{ct})(0.7)(f_{ctm}(t))}{\gamma_c} \quad (6)$$

where  $\alpha_{ct}$  is a coefficient accounting for long term effects on tensile strength,  $f_{ctm}(t)$  is the tensile strength and  $\gamma_c$  is a partial safety factor.

Section 8.10.2.2 (1) states that other values of  $\eta_{p1}$  may be used for other alternative types of tendons other than those given above (subject to a European Technical Approval). The value of  $\eta_1$  (Eq. 5) will be taken as 0.7 as a worst case scenario. Regarding a value for  $f_{ctm}(t)$ , an estimate will be made in this calculation for gunite based on inspections of actual

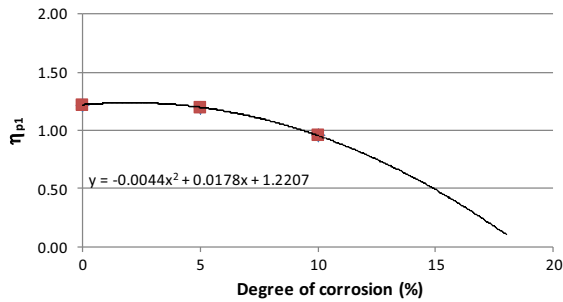


**Fig. 5** Reduction in  $\eta_{p1}$  with increasing corrosion (unfactored)

pre-load structures (on-site evaluations conducted previously determined that pneumatic gunite was approximately Grade 35 with a cement content of 340 kg/m<sup>3</sup>). In Table 3.1 of EC 2 [14],  $f_{ctm}(t)$  for a Grade 35 concrete is 3.2 N/mm<sup>2</sup>, so in this analysis, a similar value will be used for the Grade 35 gunite for analytical purposes. The coefficient  $\alpha_{ct}$  takes account of long term effects on the tensile strength and of unfavourable effects, resulting from the way the load is applied, and the recommended value is 1.0. Factor of safety,  $\gamma_c$ , is 1.5 from EC 2, Section 2.4.2.4 [14] (although for research purposes, this will be taken as 1.0). Therefore,  $f_{ctd}(t)$  is calculated as:

$$f_{ctd}(t) = (1.0)(0.7)(3.2)/1.0 \quad (7)$$

to give  $f_{ctd}(t) = 2.24$  (unfactored). Therefore, substituting these values into Eq. 5 gives

$$f_{bpt} = (\eta_{p1})(0.7)(2.24). \quad (8)$$

Referring to Table 1, the average bond stress at pre-stress transfer,  $f_{bpt}$  (rupture of the tendons) is 1.91 N/mm<sup>2</sup> at 0% corrosion, 1.88 N/mm<sup>2</sup> at 0–5% corrosion and 1.50 N/mm<sup>2</sup> at 5–10%. Substituting these values

for  $f_{bpt}$  into Eq. 8 gives empirical values for  $\eta_{p1}$  as shown graphically in Fig. 5. Referring to Fig. 5, once an estimate of the degree of corrosion is obtained from a field investigation,  $\eta_{p1}$  can be obtained from Fig. 5.

In this analysis, it is assumed that at 0% corrosion, the galvanising is generally in a very good condition but rupture has occurred due to very localised corrosion. This is likely to be the situation for most pre-load structures (see Fig. 6) but nevertheless, if widespread corrosion is present,  $\eta_{p1}$  can be estimated accordingly from Fig. 5. For comparison, the minimum value of  $\eta_{p1}$  (for indented wires) is 2.7 in EC 2 [14], hence this paper recommends a reduced value of 1.22 for smooth, uncorroded galvanised tendons. The combination of the smoothness of galvanising, corrosion and dry-spray gunite, therefore, reduces the bond characteristics at transfer (rupture of the tendons) compared to concrete and indented wires and this has implications on the transmission length as shown in the next section. The value for bond stress determined (e.g.  $f_{bpt} = 1.91$  N/mm<sup>2</sup> for uncorroded tendons) will

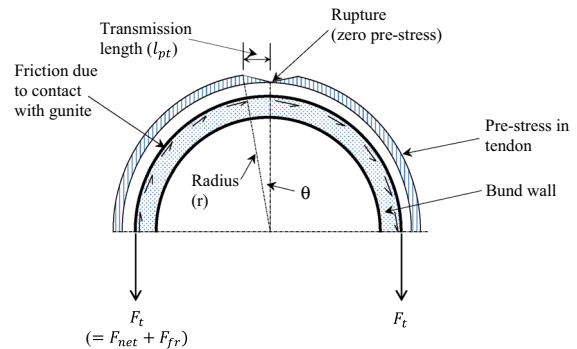


**Fig. 7** Plan of half bund wall with pre-stressed single tendon

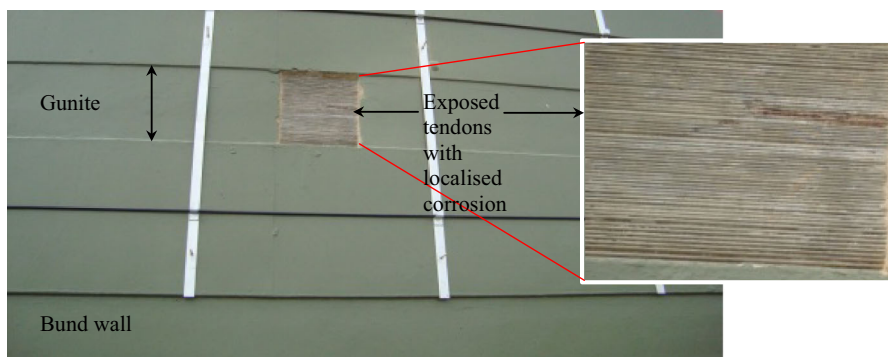
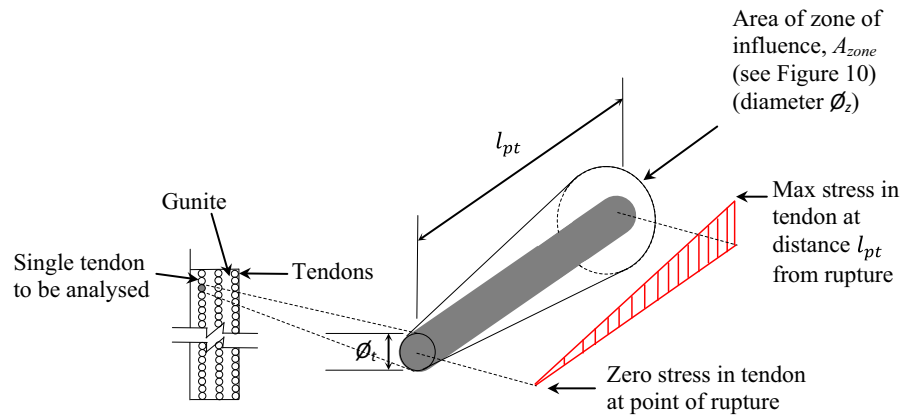


**Fig. 6** Typical bund wall with exposed tendons

**Fig. 8** Idealised section through pre-stressing recess



be used in the next section to establish the influence of frictional resistance between the tendon and the gunite.

## 5.2 Frictional resistance at tendon/gunite interface

An additional resistance is possible in the transmission length due to the friction generated at the interface of the tightly wrapped tendon and gunite. This is as a result of the lateral component of the pre-stressing force due to the curvature of the tendon. Referring to Fig. 6, an example of exposed tendons is shown as the gunite cover has been removed from the tendon recess. Referring to Fig. 7, a plan view (not to scale) of half of a bund wall is shown.

The pre-load force in the tendon is  $F_t$  (right hand side). Assuming the tendon is wound in an anticlockwise direction, the total force on the left hand side is also  $F_t$  but can be split to give  $F_{net}$ , the net force in the tendon after frictional losses and  $F_{fr}$ , the loss in force due to friction. The pre-stress in the tendon is also shown in Fig. 7 (uniformly for simplicity, although in reality, it will decrease ever so slightly due to the frictional losses as the tendon is wound in an anticlockwise direction).

The tendon recess (Fig. 6) is shown idealised in Fig. 8 where a number of vertical layers of tendons with gunite cover between them is shown. The depth and length of the recess can vary from structure to structure, but in the bunds inspected by the authors<sup>1</sup>, the number of tendons varied from about 240–370 for a depth of 80 mm and height around 500 mm (bund wall thickness was 500 mm). A tendon in the outermost layer is assumed to rupture as this will be a worst case scenario (an explosive failure is more likely at

this location as inner tendons will have more confinement, corrosion is also more likely on the outer layer).

When the tendon ruptures, the pre-stress becomes zero at the point of failure but gradually increases along the transmission length ( $l_{pt}$ , Figs. 7, 8). The pre-stressing force ( $F_t$ ) is fully mobilised beyond  $l_{pt}$  and transmitted to the gunite via bond. This is shown in Fig. 8 where a single tendon is isolated to clarify the transmission length,  $l_{pt}$ , and increasing stress from point of rupture (zero stress) to full pre-stress at a distance  $l_{pt}$ . From EC 2 [14], the transmission length,  $l_{pt}$ , is given by:

$$l_{pt} = (\alpha_1)(\alpha_2)(\phi_t)(\sigma_{pm0})/f_{bpt} \quad (9)$$

where  $\alpha_1 = 1.25$  for sudden release,  $\alpha_2 = 0.25$  for tendons with circular cross section and  $\phi_t$  is nominal diameter of tendon (5 mm).

$\sigma_{pm0}$  is the tendon stress just after release (in the bund walls inspected by the authors<sup>1</sup>, the pre-load was the equivalent of 1.5 metric tonnes (14,710 N)<sup>1</sup>,  $f_{bpt}$  is the constant bond stress at pre-stress transfer (1.91 MPa from Sect. 5.1 for 0% corrosion).

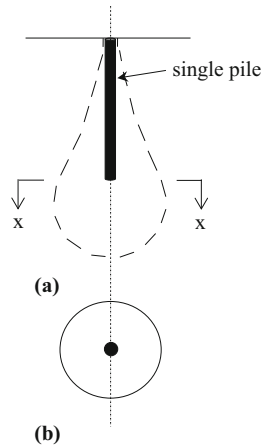
Inserting the above values into Eq. 9 gives:

$$l_{pt} = (1.25)(0.25)(5)(14,710/19.63)/1.91 \quad (10)$$

or  $l_{pt} = 613$  mm. No factors of safety e.g. 1.5 for concrete are included but regardless, the transmission

<sup>1</sup> In conventional pre-stressed concrete, there are a number of effects which cause a loss in pre-stress, such as elastic shortening of the concrete, shrinkage and creep of concrete, frictional loss, relaxation of steel and anchorage take-up. However, in the pre-load technique, only the latter three would apply but for simplicity in calculation, a pre-load of 1.5 metric tonnes is assumed without any losses as a worst case scenario.

**Fig. 9** **a** Vertical section through pile pressure bulb, **b** horizontal section  $x$ – $x$  through pile pressure bulb



length, with or without factors of safety is easily achievable due to the vast size of such bund wall structures (the bund wall previously inspected had an outer circumference of 198 m). A longer transmission length in this case can be beneficial as the pre-stress transfer slowly builds up over  $l_{pt}$  to reach the maximum stress (Fig. 8).

Referring to Fig. 7, it is assumed the tendon is wrapped in an anticlockwise direction. The frictional resistance encountered between the tendon and gunite in the transmission length can be analysed using the equation for post-tensioning loss due to curvature as follows [18]:

$$F_{net} = (F_t)(e^{-\mu\theta}) \quad (11)$$

where  $F_{net}$  is the net force in the tendon after frictional losses  $F_t$  is the pre-load force in the tendon,  $\mu$  is the coefficient of friction between steel and gunite, taken

as 0.57 [19],  $\theta$  is the subtended angle in radians where  $r = 31.5$  m (therefore  $l_{pt}/r = 613/31,500 = 0.019$ .)

Therefore, substituting these values into Eq. 11 gives:

$$F_{net} = (14,710)e^{-(0.57)(0.019)} \quad (12)$$

or  $F_{net} = 14,552$  N. Therefore, the loss in force due to frictional resistance as a result of the insignificant curvature,  $F_{fr}$ , is only 158 N ( $F_t - F_{net}$ ) over the transmission length of 613 mm and as a result, can be ignored. This will not significantly reduce the pre-load transfer of 14,710 N to the gunite at rupture.

### 5.3 Stress in gunite at single tendon rupture

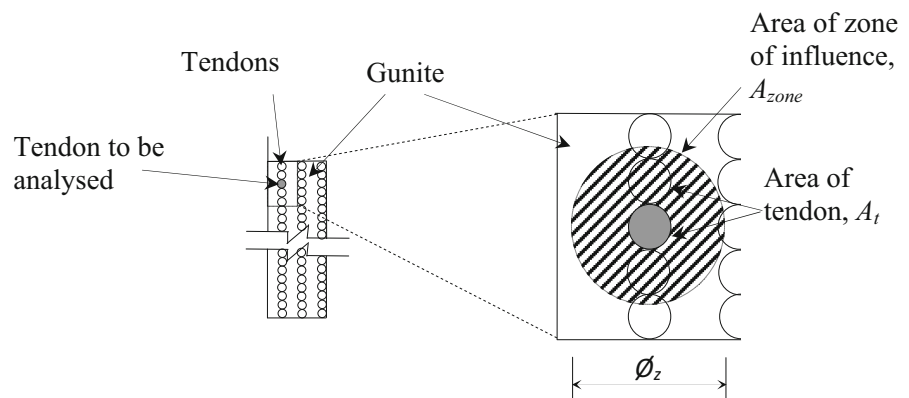
Referring to Figs. 7 and 8, the zero stress at point of rupture will increase gradually along the tendon until full pre-load is transferred to the gunite at the end of the transmission length ( $l_{pt}$ ). At this point, the force in the gunite ( $F_g$ ) equals the force in the tendon ( $F_t$ ) due to equilibrium and since force equals stress times area, it follows that:

$$f_g A_{zone} = f_t A_t \quad (13)$$

where  $f_g$  and  $f_t$  are the stresses in the gunite and tendon respectively and  $A_{zone}$  is the area of the influenced zone and  $A_t$  is the area of the tendon.

It is well known that the design strength of concrete has a factor of safety,  $\gamma_c$ , of 1.5 (or 67% of characteristic strength [14]) but since the likelihood of errors are higher in sprayed gunite, a higher factor of safety was proposed. Most gunites are likely to have a ‘design’ strength in the range 30–35 N/mm<sup>2</sup> but there could be instances where operators did not get

**Fig. 10** Idealised area of zone of influence due to single tendon rupture



the water content correct or insufficient curing was conducted. This could lead to a weaker than expected gunite. Therefore, the permissible stress in the gunite will be limited to say  $45\% f_{cu}$ , selected on the basis of a similar pre-compression in the concrete of the bund wall. Hence:

$$f_g = 0.45f_{cu} \quad (14)$$

Substituting Eq. 14 into 13 and rewriting in terms of  $A_{zone}$  gives:

$$A_{zone} = \frac{f_t A_t}{0.45f_{cu}} \quad (15)$$

In the example, using  $f_t = 750 \text{ N/mm}^2$  from a pre-load of 1.5 metric tonnes,  $A_t = 19.6 \text{ mm}^2$  for a 5 mm diameter tendon and  $0.45f_{cu}$  equal to  $15.8 \text{ N/mm}^2$ , the area of gunite,  $A_g$ , required for equilibrium is  $935 \text{ mm}^2$  from Eq. 15.

In order to estimate the area of gunite in the idealised section that is influenced by the ruptured tendon, an analogy is made with the pressure exerted on adjacent soil through a loaded single pile. Referring to Fig. 9a, the adjacent soil is stressed in the shape of a bulb if a vertical section (y–y) is taken along its depth. However, if a horizontal section (x–x, Fig. 9b) is taken, the stress is distributed uniformly around the pile in a circular shape. Therefore, it will be assumed that when a tendon ruptures, the zone of the influenced gunite can also be assumed as circular in the vertical plane commencing at a distance  $l_{pt}$  (Fig. 8).

Referring to Fig. 10, a section through the recess is given which highlights the zone of influence,  $A_{zone}$ , as a result of the ruptured tendon. This circular area will overlap and/or intersect adjacent tendons above and below the ruptured tendon under consideration which will contribute to carrying the compressive force in the gunite. The area of the zone of influence,  $A_{zone}$ , is calculated from:

$$A_{zone} = [A_{ring} - nA_t] + A_{g(equiv)} \quad (16)$$

where  $A_{ring}$  is the area of a circular ring, inner diameter 5 mm (diameter of the ruptured tendon) and an outer diameter  $\phi_z$  but minus the area of the other unruptured tendons within it (i.e.  $nA_t$ ). However, since these tendons will help absorb the pre-stress transfer, they can be converted to an equivalent area of gunite,  $A_{g(equiv)}$ , using the modular ratio ( $m$ ) between the tendon and gunite ( $E_t$  and  $E_g$  respectively),  $nmA_t$ .

where  $n$  is the number of tendons in the zone of influence. Equation 16 can be expanded to:

$$A_{zone} = \left[ \frac{\pi\phi_z^2}{4} - \frac{\pi\phi_t^2}{4} \right] - n \frac{\pi\phi_t^2}{4} + nm \frac{\pi\phi_t^2}{4} \quad (17)$$

where  $\phi_z$  is the diameter of the zone of influence and  $\phi_t$  is the diameter of the tendon. From Eq. 15, the area of the zone of influence ( $A_{zone}$ ) for equilibrium is  $935 \text{ mm}^2$ .

Substituting this into Eq. 17, taking  $\phi_t$  as 5 mm,  $m = 14.5$  and rearranging gives:

$$\frac{\pi\phi_z^2}{4} = 935 + 19.6 - n(303) \quad (18)$$

Simplifying Eq. 18 in terms of  $\phi_z$  gives:

$$\phi_z = \sqrt{1216 - 386n} \quad (19)$$

However, Eq. 19 is indeterminate since the diameter in the zone of influence (left hand side of equation) is a function of the number of tendons within the zone and cannot be solved directly. A second equation, therefore, is proposed which directly relates the number of tendons within the diameter  $\phi_z$  (see Fig. 10) where  $n$  is the number of tendons in the zone of influence. However, the diameter of the ruptured tendon will also form part of the diameter,  $\phi_z$  giving a total number of tendons  $n + 1$ . Therefore:

$$\phi_z = \phi_t(n + 1) \quad (20)$$

Equating Eqs. 19 and 20 gives:

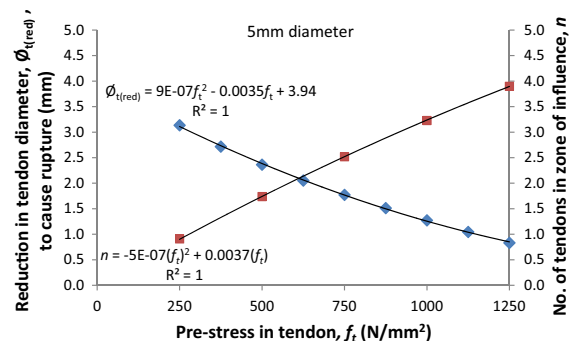
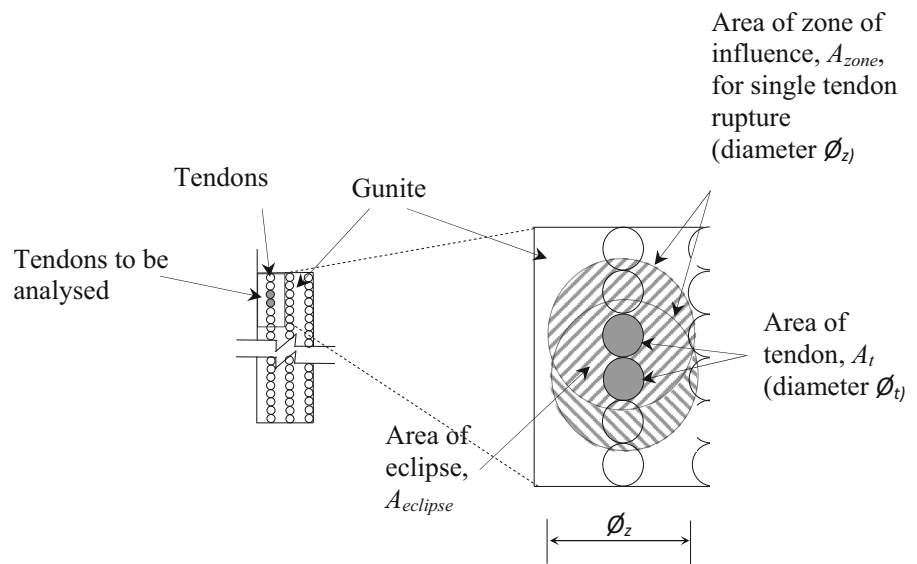


**Fig. 11** Determination of: (primary y-axis) loss in ruptured tendon diameter for different levels of pre-stress transfer; (secondary y-axis) number of 5 mm  $\phi$  tendons in zone of influence for other levels of pre-stress transfer

**Fig. 12** Idealised area of zones of influence due to double tendon rupture



$$\sqrt{1216 - 386n} = \phi_t(n + 1) \quad (21)$$

Substituting  $\phi_t = 5$  mm and squaring both sides of Eq. 21 gives:

$$1216 - 386n = [5(n + 1)]^2 \quad (22)$$

Expanding Eq. 22 gives:

$$1216 - 386n = 25n^2 + 50n + 25 \quad (23)$$

Simplifying Eq. 23 gives a quadratic equation in the form:

$$25n^2 + 436n - 1191 = 0 \quad (24)$$

and solving gives the positive root as 2.4, meaning the number of tendons in the zone of influence,  $n$ , is 2.4 (or 3.4 if the ruptured tendon is included). Inserting  $n = 2.4$  back into Eq. 19 (or Eq. 20) gives  $\phi_z = 17$  mm, the diameter of the zone of influence (Fig. 10). The cover,  $C_t$ , to the ruptured tendon can now be checked from:

$$C_t = \frac{\phi_z}{2} - \frac{\phi_t}{2} \quad (25)$$

which, as  $\phi_z = 17$  mm and  $\phi_t = 5$  mm in this instance, gives  $C_t = 6$  mm. Therefore, a cover to the tendon of at least 6 mm means that there will be sufficient gunit to absorb the pre-stress transfer from a ruptured tendon and the permissible stress will not be exceeded. The likelihood of an explosive failure will be avoided. The actual cover in a real bund wall can be determined by

conducting a covermeter survey [20] and highlighting areas where low cover is present. However, a half cell survey [21] would commonly be used to identify areas where corrosion hotspots are likely but in this instance, the zinc galvanising on the tendons would render the technique unworkable (ASTM C876 standard indicates that the zinc protects the steel reinforcement and the measured half cell potential reading is no longer the corrosion potential of the steel reinforcement but the mixed potential of steel and zinc [22]). Other techniques such as magnetic flux leakage are gaining ground but are more useful for inspecting plates and pipes [23] and not yet full established for this use. The key information for the inspection engineer is that an explosive failure is possible if a combination of low cover (say less than 5 mm) and corrosion is present, based on the pre-stress transfer of a single ruptured tendon in this example.

If low cover is an issue, an indication of the level of deterioration required before a tendon is at risk of rupturing can be determined from the following simple analysis. In the example presented here, the pre-load ( $F_t$ ) of 14,710 N (1.5 metric tonnes) was carried on a tendon with a diameter of 5 mm, giving a working pre-stress of 750 N/mm<sup>2</sup>. To get an indication of the reduction in tendon diameter before stress levels reach ultimate levels, typically 1800 N/mm<sup>2</sup> ( $f_{t(uts)}$ ) for high strength tendons, the following equation can be employed:



$$\frac{\pi \phi_{t(\text{corr})}^2}{4} = \frac{F_t}{f_{t(\text{uts})}} \quad (26)$$

where  $\phi_{t(\text{corr})}$  is the reduced diameter of the corroded tendon. Substituting known values into Eq. 26 and simplifying gives:

$$\phi_{t(\text{corr})} = 3.22 \text{ mm} \quad (27)$$

Therefore, a reduction in tendon diameter ( $\phi_{t(\text{red})}$ ) of 1.78 mm i.e.  $\phi_t - \phi_{t(\text{corr})}$  would be required for failure to occur due to overstressing in this example. A loss in tendon diameter of this magnitude would be possible by a combination of general and pitting corrosion. For comparison, the tendon in Fig. 3b (albeit 5.4 mm in diameter) exhibiting 6% loss of cross sectional area would have a loss in diameter ( $\phi_{t(\text{red})}$ ) of 0.16 mm assuming uniform loss of section. However, in reality, pitting corrosion will be the main concern for the inspection engineer as it is not possible with existing techniques to establish where deep pits occur and these cause significant loss in tendon diameter which greatly increase the risk of rupture.

The example presented here focuses of a pre-load of 1.5 metric tonnes on the tendon (giving a pre-stress,  $f_t$ , of 750 N/mm<sup>2</sup>). However, if the design pre-stress varies in the ruptured tendon, the loss in diameter to cause failure also varies. This is considered in Fig. 11 where  $F_t$  is varied in Eq. 26 to give different levels of pre-load in the tendon (converted to pre-stress,  $f_t$ , in Fig. 11). The reduction in tendon diameter,  $\phi_{t(\text{red})}$  (primary y-axis in Fig. 11) can be related to the pre-stress in the tendon by:

$$\phi_{t(\text{red})} = 9E - 07f_t^2 - 0.0035f_t + 3.94 \quad (28)$$

As an example, it was reported earlier that a reduction in cross-sectional area of a wire can exceed 30% after only 20 years of corrosion propagation even at low corrosion rates [2]. A 30% loss of cross sectional area would reduce a 5 mm diameter tendon by 0.82 mm. Inserting  $\phi_{t(\text{red})} = 0.82$  mm into Eq. 28 and solving the quadratic equation yields a pre-stress ( $f_t$ ) of 1384 N/mm<sup>2</sup>. This means a pre-stress of 1384 N/mm<sup>2</sup> coupled with a loss in diameter of 0.82 mm would lead to an ultimate stress of 1800 N/mm<sup>2</sup> being achieved in the tendon. However, a pre-stress of this magnitude would give a stress/strength ratio of 77% (1384/1800 N/mm<sup>2</sup>) in-service, so is on the high side as maximum stress levels in tendons would normally be about 60%,

but nevertheless, highlights the risk of rupture due to a combination of corrosion and high pre-stress in the tendon.

In addition, rupture of tendons at other levels of pre-stress will also influence the diameter of the zone of influence,  $\phi_z$ , Fig. 10. This is also modelled in Fig. 11 where the number of tendons,  $n$  (secondary y-axis) contributing to absorbing the pre-stress transfer in the gunite can be determined from the pre-stress in the tendon. From the line of best fit,  $n$  can be determined from:

$$n = -4E - 07(f_t)^2 + 0.0035(f_t). \quad (29)$$

Once  $n$  is known from Eq. 29 for a specific pre-stress,  $\phi_z$  can be determined as before from Eq. 15 (or Eq. 20) and the cover,  $C_t$ , can be determined from Eq. 25. As an example, if a tendon with a higher pre-stress of say 1250 N/mm<sup>2</sup> ruptured, a minimum cover ( $C_t$ ) of 9.4 mm would be required for the gunite to absorb the compressive stress (as opposed to 6 mm for a pre-stress transfer of 750 N/mm).

This analysis assumes that the strength of the gunite,  $f_{cu}$ , is constant at 35 N/mm<sup>2</sup> and the diameter of the tendon,  $\phi_t$ , is 5 mm with  $E_t = 289$  and  $E_g = 20$  kN/mm<sup>2</sup> respectively which is considered typical for this type of construction. However, if these properties were to change, Eqs. 9–25 can, nevertheless, be used with the new values to determine the stress in the gunite and minimum cover required.

#### 5.4 Stress in gunite at two or more tendon ruptures

Since corrosion can be very localised (see Fig. 6), it is possible for two or more adjacent tendons to suffer damage at a similar point along their circumference, hence there is a possibility of overstressing the gunite due to double (or more) pre-stress transfer. Referring to Fig. 12, the gunite area of influence overlaps for two adjacent tendons. It is assumed that both tendons do not rupture at exactly the same time, it is more likely that one will rupture first followed by the second sometime later, hence the concept of pre-stress transfer influencing a zone around the single tendon as analysed in Sect. 5.3 also applies here. Referring to Eq. 15, the area of gunite required for equilibrium for a single tendon rupture in this example is 935 mm<sup>2</sup> ( $A_{\text{zone}}$ ), hence this will be doubled to 1870 mm<sup>2</sup> at double tendon failure ( $2A_{\text{zone}}$ ). However, the zone of



influence from two ruptured adjacent tendons will overlap (Fig. 12) meaning the eclipsed area will be subjected to two pre-stress transfers and possible over stressing. Using  $\phi_z = 17 \text{ mm}$  from Eq. 16 or 20, the eclipsed area ( $A_{\text{eclipse}}$ ) is  $143 \text{ mm}^2$  from [24]. However, this area will include tendons which will also help carry the pre-stress transfer and by inspection of Fig. 12, the adjacent zone of influence due to the second tendon rupture has moved downwards by one tendon diameter. It was established above (Eq. 24 or 29) that  $n$  equals 2.4 tendons in a single zone of influence, hence  $n$  in the eclipsed area will be one tendon diameter less or 1.4 (this includes the tendon which ruptured first as this will now support the pre-stress transfer to the gunite). Since the area of the eclipsed zone of influence ( $A_{\text{eclipse}}$ ) equals  $143 \text{ mm}^2$  from above, the net area of gunite in the eclipsed zone ( $A_{g(\text{eclipse})}$ ) will be  $A_{\text{eclipse}}$  minus the area of the tendons within this zone i.e.  $nA_t$  or  $1.4A_t$ . As shown in Sect. 5.3, these tendons will contribute to carrying the pre-stress so an equivalent area of gunite ( $A_{g(\text{equiv})} = nmA_t$ ) can be obtained to give:

$$A_{g(\text{eclipse})} = A_{\text{eclipse}} - nA_t + nmA_t \quad (30)$$

Substituting known values into Eq. 30 gives:

$$A_{g(\text{eclipse})} = 143 - 28 + 397 \quad (31)$$

or  $A_{g(\text{eclipse})} = 512 \text{ mm}^2$ . Modifying Eq. 15 and rewriting gives an estimate of the stress in the eclipsed zone of influence due to the second tendon rupture:

$$f_{g(\text{eclipse})} = \frac{f_t A_t}{A_{g(\text{eclipse})}} \quad (32)$$

Inserting known values ( $f_t = 750 \text{ N/mm}^2$ ,  $A_t = 19.6 \text{ mm}^2$  and  $A_{g(\text{eclipse})} = 512 \text{ mm}^2$ ) gives  $f_{g(\text{eclipse})} = 28.8 \text{ N/mm}^2$ . This is the additional pre-stress transferred to the gunite in the eclipsed zone of influence. In the analysis, it was assumed that the permissible stress in the gunite,  $f_g$  is  $0.45f_{cu}$ , or  $15.8 \text{ N/mm}^2$  (Eq. 14). The additional stress in the gunite in the eclipsed zone,  $f_{g(\text{eclipse})}$ , is  $28.8 \text{ N/mm}^2$  meaning a combined stress of  $44.6 \text{ N/mm}^2$  and, therefore, greater than the strength of the gunite ( $35 \text{ N/mm}^2$ ). In this case, failure of the gunite is likely and an explosive failure is possible, hence caution should be exercised.

## 6 Conclusions

The following are the conclusions emanating from the laboratory study and associated analysis of the pre-stress transfer of ruptured galvanised tendons in bund walls and storage tanks:

1. A reduced value of 1.22 for coefficient  $\eta_{p1}$ , the coefficient that takes into account the type of tendon and the bond situation in Eurocode 2, is proposed for smooth, galvanised uncorroded tendons. Where corrosion is present, a further reduction in  $\eta_{p1}$  to 1.20 and 0.96 is proposed for degrees of corrosion (loss in cross sectional area) up to 5 and 10% respectively.
2. Frictional resistance due to curvature between the ruptured tendon and gunite in the transmission length can be ignored for pre-load bund walls and storage tanks with large diameters.
3. The area of the zone around a ruptured tendon,  $A_{\text{zone}}$ , can be determined from  $A_{\text{zone}} = \frac{\pi\phi_z^2}{4} - \frac{\pi\phi_t^2}{4} + nm\frac{\pi\phi_t^2}{4}$  from which an expression for the diameter of the zone of influence,  $\phi_z$ , can be obtained. A second expression for the diameter of the same zone around a single ruptured tendon can be obtained from  $\phi_z = \phi_t(n+1)$ .
4. The number of tendons in the zone of influence can be determined by equating  $\frac{\pi\phi_z^2}{4} - \frac{\pi\phi_t^2}{4} + nm\frac{\pi\phi_t^2}{4}$  with  $\phi_t(n+1)$  and solving the resultant quadratic equation.
5. The gunite cover to the ruptured tendon can be determined from  $C_t = \frac{\phi_z}{2} - \frac{\phi_t}{2}$ . If the actual gunite cover on the wrap around tendons in a tank or bund wall is less than  $C_t$ , then the permissible stress in the gunite will be exceeded due to insufficient area to absorb the pre-stress transfer.
6. A reduction in diameter due to corrosion of 1.78 mm in a 5 mm diameter tendon would lead to over stressing and possible failure of the tendon.
7. Double rupture of two adjacent tendons with a pre-stress of  $750 \text{ N/mm}^2$  is likely to cause over-stressing and possible explosive failure of the gunite.

**Acknowledgements** The Authors' wish to thank the financial contribution made by Mott MacDonald for the laboratory element of this study. They would also like to thank Bridon Wire Ltd. for supplying the galvanized tendons for use in this



research. The use of images from the metallurgical analysis conducted by ESR Technology (Fig. 3) is also appreciated.

### Compliance with ethical standards

**Conflict of interest** The authors declare that they have no conflict of interest.

### References

- Crom JM (2017) Method and apparatus for banding tanks, March 6, 1945. Patent No. 2,370,780, <http://www.google.sr/patents/US2370780>. Accessed 5 Sept 2017
- Darmawan MS, Stewart MG (2007) Effect of pitting corrosion on capacity of prestressing wires. *Mag Concr Res* 59(2):131–139. DOI <https://doi.org/10.1680/mac.2007.59.2.131>
- Yang WJ, Yang P, Li XM, Feng WL (2012) Influence of tensile stress on corrosion behaviour of high-strength galvanized steel bridge wires in simulated acid rain. *Mater Corros* 63(5):401–407. doi:10.1002/maco.201005921
- Gaillet L, Recio FJ, Alonso MC, Sánchez M (2011) Hydrogen embrittlement risk of high strength galvanized steel in contact with alkaline media. *Corros Sci* 53:2853–2860. doi:10.1016/j.corsci.2011.05.023
- Short NR, Zhou S, Dennis JK (1996) Electrochemical studies on corrosion of a range of zinc alloy coated steel in alkaline solutions. *Surf Coat Tech* 79:218–224. doi:10.1016/0257-8972(95)02428-X
- Andrade C, Alonso C (2004) Electrochemical aspects of galvanized reinforcement corrosion. In: Yeomans SR (ed) *Galvanised steel reinforcement in concrete*. Oxford University Press, Oxford, pp 111–144
- Yeomans SR (2004) *Galvanised steel reinforcement in concrete*. Elsevier, Oxford, pp 1–293
- Nürnberg U (2006) Corrosion of metals in contact with mineral building materials. In: Raupach M, Elsener B, Polder R, Mietz J (eds) *Corrosion Reinforcements in Concrete* (EFC 38). EFC series, Belgium, pp 1–336
- Wu Y, Nürnberg U (2009) Corrosion-technical properties of high-strength stainless steels for the application in pre-stressed concrete structures. *Mater Corros* 60:771–780. doi:10.1002/maco.200905279
- Menzel K (2007) Proc of 3-Länder-Korrosionstagung, Stuttgart, Germany, April 18–19, pp 59–67
- Mietz J, Rückert J (1997) Electrochemical investigations of high strength Stainless steels for rock and ground anchors. *Mater Corros* 48(6):353–363. doi:10.1002/maco.19970480603
- Helene P, Ferreira MF, Castro P (2004) Performance of 40-year old concrete bridge with embedded prestressed galvanized strands. *Mater Perform* 43(10):42–45
- Bladon S (2009) Repair techniques for prestressed concrete tanks. *J Protect Coat Linings*; Pittsburgh: 45–47. [http://www.paintsquare.com/library/articles/repair\\_techniques\\_for\\_prestressed\\_concrete\\_tanks.pdf](http://www.paintsquare.com/library/articles/repair_techniques_for_prestressed_concrete_tanks.pdf). Accessed 30 June 2017
- British Standards Institution (2014). Eurocode 2: Design of concrete structures—Part 1-1: General rules and rules for buildings, BS EN 1992-1-1:2004 + A1:2014
- Elliott KS (2014) Transmission length and shear capacity in prestressed concrete hollow core slabs. *Mag Concr Res* 66(12):585–602. doi:10.1680/mac.13.00251
- British Standards Institution (2013) *Aggregates for concrete*. BS EN 12620:2013
- O’Flaherty FJ, Mangat PS, Lambert P, Browne EH (2008) Effect of under reinforcement on the flexural strength of corroded beams. *Mater Struct* 41:311–321. doi:10.1617/s11527-007-9241-1
- Mosley WH, Bungey JH (1992) *Reinforced concrete design*. Fourth Edition. Palgrave, London
- Rabbat BG, Russell HG (1985) Friction coefficient of steel on concrete or grout. *J Struct Eng* 111(3):505–515. doi:10.1061/(ASCE)0733-9445(1985)111:3(505)
- British Standards Institution (1988). *Testing concrete. Recommendations on the use of electromagnetic covermeters*, BS 1881-204
- The Concrete Society, Half-cell potential surveys, Current Practice Sheet 120, Concrete, July/August 2000
- Gu P, Beaudoin JJ (1998) Obtaining effective half-cell potential measurements in reinforced concrete structures, *Construction Technology Update*, No. 18, July 1998. [https://www.nrc-cnrc.gc.ca/ctu-sc/ctu\\_sc\\_n18](https://www.nrc-cnrc.gc.ca/ctu-sc/ctu_sc_n18). Accessed 5 Sept 2017
- Drury JC, Marino A (2000) A comparison of the magnetic flux leakage and ultrasonic methods in the detection and measurement of corrosion pitting in ferrous plate and pipe. In: 15th WCNDT, Rome 2000, [www.ndt.net/article/wcndt00/papers/idn701/idn701.htm](http://www.ndt.net/article/wcndt00/papers/idn701/idn701.htm) [Accessed 5 Sep 2017]
- Lune calculator, <https://rechneronline.de/pi/lune.php>. Accessed 11 July 2017

